# Renin Inhibitory Peptides. A β-Aspartyl Residue as a Replacement for the Histidyl Residue at the P-2 Site†

Suvit Thaisrivongs,*,‡ Boryeu Mao,§ Donald T. Pals,‡ Steve R. Turner,‡ and Lisa T. Kroll‡

*Cardiovascular Diseases Research and Computational Chemistry, The Upjohn Company, Kalamazoo, Michigan 49001.*
*Received August 31, 1989*

In an effort to decrease the size and to increase the hydrophilicity of the previously prepared renin inhibitory peptides, it was postulated that one might be able to take advantage of the polar Thr-84 on the flap region of the enzyme renin by potential hydrogen bonding to polar functionality on the inhibitory peptide at the P-2 site. A β-aspartyl residue with a carboxylic acid group was proposed to be a possible replacement for the histidyl residue at the P-2 site. A series of renin inhibitory peptides were prepared with the β-aspartyl residue to probe the structure–activity relationship of the resulting peptides. Potent inhibitory peptides could be realized with activity in the subnanomolar range. Molecular modeling was also undertaken to investigate the interactions between the enzyme active site and the new inhibitors and to suggest a possible mode of binding of these ligands to the enzyme. From this modeling study, the role of Ser-229 at the active site in the bound conformer of the inhibitors was suggested. It was further noted in the analogue study that a malic acid residue, which is the oxygen analogue of the β-aspartic acid residue, could lead to further enhancement of inhibitory potency of congeneric peptides. Small renin inhibitors, such as compound XII with molecular weight 535 and with no α-amino acid residue, could be prepared and exhibited renin inhibitory activity in the nanomolar range.

The renin–angiotensin system has been implicated in several forms of hypertension.[1] Renin catalyzes the first and rate-limiting step of the enzymatic cascade by cleaving the polypeptide substrate, angiotensinogen, to form the decapeptide intermediate angiotensin I. This decapeptide is further cleaved by angiotensin converting enzyme to yield the biologically active octapeptide angiotensin II. This octapeptide causes vasoconstriction and stimulates secretion of aldosterone and catecholamine, leading to elevation of blood pressure. The uniquely high specificity of renin offers the potential of specific pharmacological intervention by its inhibitors.[2] Interest in the blockade of renin has led to the rapid development of potent inhibitors as potential antihypertensive agents by analogues of the substrate angiotensinogen. The most successful approach has been based on the concept of transition-state analogues of the catalytic mechanism.[3] Modification at the cleavage site to mimic the tetrahedral species of the peptidic bond have generated analogues of the minimum substrate with very high inhibitory potency in vitro.[4]

Many renin inhibitors have been shown to lower blood pressure in renin-dependent animal models by intravenous administration and also by the oral route.[5] Efforts to discover inhibitors with longer duration of action and higher oral bioavailability continue to make progress.[6] Current research programs focus on decreasing the size of these renin inhibitors and changing the physical characteristics of these lipophilic compounds in order to improve the oral absorption and to slow down hepatic clearance of the resulting compounds.

We have initiated a program with the intention of addressing the stability of these peptidic compounds against proteolytic degradation[7] in an attempt to discover compounds with increased duration of action in vivo. In our previous reports, we have described our work on peptide backbone modifications and demonstrated the feasibility of orally active renin inhibitory peptides[8] from this approach. We had chosen to examine the peptidic bond between the amino acids at the P-2 and P-3 sites[9] in these peptides as a likely point of cleavage by proteolytic enzymes. The present study discusses a continuation of our work with emphasis on an increase in hydrophilicity and a decrease in the size of the resulting peptides.

**Table I.** Inhibition of Human Plasma Renin

| | | $IC_{50}$, nM |
|---|---|---|
| I | $C_6H_5CH_2CO$-His-Leu$^{OH}$Val-Ile-Amp | 220 |
| II | $C_6H_5CH_2CO$-β-Asp-Leu$^{OH}$Val-Ile-Amp | 3.5 |
| III | $C_6H_5CH_2CO$-β-D-Asp-Leu$^{OH}$Val-Ile-Amp | 17 |
| IV | $C_6H_5CH_2CO$-β-Asp-Cal$^{OH}$Val-Ile-Amp | 2.0 |
| V | $C_6H_5OCH_2CO$-His-Leu$^{OH}$-Val-Ile-Amp | 8.5 |
| VI | $C_6H_5OCH_2CO$-β-Asp-Leu$^{OH}$Val-Ile-Amp | 1.9 |
| VII | $C_6H_5OCH_2CO$-β-Asp-Cal$^{OH}$Val-Ile-Amp | 0.34 |
| VIII | $C_6H_5OCH_2CO$-β-Asp-Leu$^{OH}$Val-Mba | 20 |
| IX | $C_6H_5OCH_2CO$-β-Asp-Cal$^{OH}$Val-Mba | 5.2 |
| X | $C_6H_5CH_2CO$-β-Mal-Leu$^{OH}$Val-Ile-Amp | 1.2 |
| XI | $C_6H_5OCH_2CO$-β-Mal-Leu$^{OH}$Val-Ile-Amp | 0.7 |
| XII | $C_6H_5CH_2CO$-β-Mal-Leu$^{OH}$Val-Mba | 6.0 |
| XIII | $C_6H_5OCH_2CO$-β-Mal-Leu$^{OH}$Val-Mba | 2.2 |
| XIV | $C_6H_5OCH_2CO$-β-Mal-Cal$^{OH}$Val-Mba | 3.6 |

During our examination of the model[10] of renin–inhibitor interaction, we were intrigued by the possibility of utilizing the polar Thr-84 on the flap region of the enzyme surface for potential hydrogen-bonding interaction with polar functionality on the inhibitors. With the desire to increase hydrophilicity of these inhibitors, we were interested in replacing the histidyl residue at the P-2 site with an amino acid residue that contains an acidic functionality for potential polar interaction with the enzyme surface. The β-aspartyl residue was proposed and both enantiomers were incorporated into an inhibitor template that con-

† Dedicated to Professor Robert E. Ireland on the occasion of his 60th birthday.

‡ Cardiovascular Diseases Research.

§ Computational Chemistry.

(1) Davis, J. O. *Circ. Res.* **1977**, *40*, 439. Swales, J. D. *Pharmacol. Ther.* **1979**, *7*, 172.
(2) Peach, M. J. *Physiol. Rev.* **1977**, *57*, 313. Ondetti, M. A.; Cushman, D. W. *Annu. Rev. Biochem.* **1982**, *51*, 283. Haber, E. *N. Engl. J. Med.* **1984**, *311*, 1631.
(3) Wolfenden, R. *Transition States of Biochemical Processes*; Gandour, R. D., Schowen, R. L.; Eds.; Plenum: New York, 1978; p 555.
(4) Boger, J. *Annu. Rep. Med. Chem.* **1985**, *20*, 257.
(5) Greenlee, W. J. *Pharm. Res.* **1987**, *4*, 364.
(6) Luther, R. R.; Stein, H. H.; Glassman, H. N.; Kleinert, H. D. *Drug Res.* **1989**, *39*, 1.
(7) Thaisrivongs, S.; Pals, D. T.; Harris, D. W.; Kati, W. M.; Turner, S. R. *J. Med. Chem.* **1986**, *29*, 2088.
(8) Pals, D. T.; Thaisrivongs, S.; Lawson, J. A.; Kati, W. M.; Turner, S. R.; Degraaf, G. L.; Harris, D. W.; Johnson, G. A. *Hypertension* **1986**, *8*, 1105.
(9) Nomenclature as described by Schechter and Berger (*Biochem. Biophys. Res. Commun.* **1967**, *27*, 157); $P_n$–$P_n'$ refer to the side-chain positions of the peptide substrate.
(10) Carlson, W.; Karplus, M.; Haber, E. *Hypertension* **1985**, *7*, 13.

0022-2623/90/1833-1337$02.50/0 

**Scheme I.** Preparation of Peptide I[a]

Boc-LeuΨ[CHOTBSCH$_2$]Val-Ile-Amp (1)

↓ a

Boc-His(Ts)-LeuΨ[CHOHCH$_2$]Val-Ile-Amp (2)

↓ b

$C_6H_5CH_2CO$-His(Ts)-LeuΨ[CHOHCH$_2$]Val-Ile-Amp (3)

↓ c

$C_6H_5CH_2CO$-His-LeuΨ[CHOHCH$_2$]Val-Ile-Amp (I)

[a] (a) HCl(g), ether; Boc-His(Ts)-OH, DEPC, $Et_3N$, $CH_2Cl_2$ (65%); (b) TFA, $CH_2Cl_2$; $C_6H_5CH_2CO_2H$, DEPC, $Pr^i_2NEt$, $CH_2Cl_2$, DMF (86%); (c) 1-HOBT, $CH_3OH$ (52%).

**Scheme II.** Preparation of Compound II[a]

Boc-LeuΨ[CHOTBSCH$_2$]Val-Ile-Amp (1)

↓ a

Boc-NHCH($CO_2Bzl$)$CH_2CO$-LeuΨ[CHOHCH$_2$]Val-Ile-Amp (4)

↓ b

$C_6H_5CH_2CO$-NHCH($CO_2Bzl$)$CH_2CO$-LeuΨ[CHOHCH$_2$]Val-Ile-Amp (5)

↓ c

$C_6H_5CH_2CO$-β-Asp-LeuΨ[CHOHCH$_2$]Val-Ile-Amp (II)

[a] (a) HCl(g), ether; Boc-β-Asp(OBzl)-OH, DEPC, $Pr^i_2NEt$, $CH_2Cl_2$ (93%); (b) TFA, $CH_2Cl_2$; $C_6H_5CH_2CO_2H$, DEPC, $Pr^i_2NEt$, $CH_2Cl_2$ (64%); (c) 10% Pd on charcoal, $HCO_2NH_4$, DMF (95%).

tained the hydroxyethylene isostere at the cleavage site of the substrate. A series of compounds were then prepared that contain the β-L-aspartyl residue to probe the structure–activity relationship of the resulting peptides. A molecular modeling study was also undertaken on the renin model, and four congeneric peptides (see Table I) were used in this study which compared the histidyl residue (compound I) to the β-L- and β-D-aspartyl (compounds II and III) and malic acid residue (compound X) at the P-2 site of these peptides.

## Chemistry[11]

As shown in Scheme I, treatment of 4(*S*)-[(*tert*-butyldimethylsilyl)oxy]-5(*S*)-[(*tert*-butyloxycarbonyl)amino]-2(*S*)-isopropyl-7-(methyloctanoyl)-L-isoleucyl-2-pyridylmethylamine (1) with hydrogen chloride in ether afforded the corresponding amine dihydrochloride, which was then coupled to (*tert*-butyloxycarbonyl)-$N^{im}$-tosyl-L-histidine to give (*tert*-butyloxycarbonyl)-$N^{im}$-tosyl-L-histidyl-5(*S*)-amino-4(*S*)-hydroxy-2(*S*)-isopropyl-7-(methyloctanoyl)-L-isoleucyl-2-pyridylmethylamine (2).[12] The *tert*-butyloxycarbonyl protecting group was removed with trifluoroacetic acid and the resulting amine was then coupled to phenylacetic acid to give (phenylacetyl)-$N^{im}$-tosyl-L-histidyl-5(*S*)-amino-4(*S*)-hydroxy-2(*S*)-isopropyl-7-(methyloctanoyl)-L-isoleucyl-2-pyridylmethylamine (3). Removal of the tosyl protecting group with 1-hydroxybenzotriazole gave the desired peptide (phenylacetyl)-L-histidyl-5(*S*)-amino-4(*S*)-hydroxy-2(*S*)-isopropyl-7-(methyloctanoyl)-L-isoleucyl-2-pyridylmethylamine (I). Compound V was also prepared in a similar manner.

β-Aspartic acid containing peptide II was prepared as shown in Scheme II. The amine dihydrochloride from 4(*S*)-[(*tert*-butyldimethylsilyl)oxy]-5(*S*)-[(*tert*-butyloxycarbonyl)amino]-2(*S*)-isopropyl-7-(methyloctanoyl)-L-isoleucyl-2-pyridylmethylamine (1) was coupled to (*tert*-butyloxycarbonyl)-α-benzyl-L-aspartic acid to give (*tert*-butyloxycarbonyl)-α-benzyl-β-L-aspartyl-5(*S*)-amino-4(*S*)-hydroxy-2(*S*)-isopropyl-7-(methyloctanoyl)-L-isoleucyl-2-pyridylmethylamine (4). The tert-butyloxycarbonyl protecting group was removed with trifluoroacetic acid and the resulting amine was then coupled to phenylacetic acid to give (phenylacetyl)-α-benzyl-β-L-aspartyl-5(*S*)-amino-4(*S*)-hydroxy-2(*S*)-isopropyl-7-(methyloctanoyl)-L-isoleucyl-2-pyridylmethylamine (5). The benzyl ester protecting group was then removed by hydrogenolysis to give the desired peptide (phenylacetyl)-β-L-aspartyl-5(*S*)-amino-4(*S*)-hydroxy-2(*S*)-isopropyl-7-(methyloctanoyl)-L-isoleucyl-2-pyridylmethylamine (II). Peptides III–IX, except peptide V, were also prepared in a similar manner.

**Scheme III.** Preparation of Compound XII[a]

Boc-LeuΨ[CHOTBSCH$_2$]Val-Mba (6)

↓ a

HOCH($CO_2Bzl$)$CH_2CO$-LeuΨ[CHOTBSCH$_2$]Val-Mba (7)

↓ b

$C_6H_5CH_2CO_2CH(CO_2Bzl)CH_2CO$-LeuΨ[CHOTBSCH$_2$]Val-Mba (8)

↓ c

$C_6H_5CH_2CO$-β-Mal-LeuΨ[CHOHCH$_2$]Val-Mba (XII)

[a] (a) TFA, $CH_2Cl_2$; 1-benzyl-(*S*)-malic acid, DEPC, $Pr^i_2NEt$, $CH_2Cl_2$ (49%); (b) $C_6H_5CH_2COCl$, DMAP, $CH_2Cl_2$ (73%); (c) TFA, $CH_2Cl_2$; 5% Pd on charcoal, $H_2$(g), $CH_3OH$ (66%).

For peptides X–XIV, the preparation of a representative peptide XII is shown in Scheme III. (*tert*-Butyloxycarbonyl)-5(*S*)-amino-4(*S*)-[(*tert*-butyldimethylsilyl)oxy]-2(*S*)-isopropyl-7-(methyloctanoyl)-2(*S*)-methylbutylamine (6) from the coupling of 4(*S*)-[(*tert*-butyldimethylsilyl)oxy]-5(*S*)-[(*tert*-butyloxycarbonyl)amino]-2(*S*)-isopropyl-7-methyloctanoic acid[7] and 2(*S*)-methylbutylamine was treated with trifluoroacetic acid to give the corresponding amine. Coupling of this amine to 1-benzyl-*S*-malic acid gave 1-benzyl-2(*S*)-malyl-5(*S*)-amino-4(*S*)-[(*tert*-butyldimethylsilyl)oxy]-2(*S*)-isopropyl-7-(methyloctanoyl)-2(*S*)-methylbutylamine (7). This hydroxyl compound was then acylated with phenylacetyl chloride to give (phenylacetyl)-1-benzyl-2(*S*)-malyl-5(*S*)-amino-4(*S*)-[(*tert*-butyldimethylsilyl)oxy]-2(*S*)-isopropyl-7-(methyloctanoyl)-2(*S*)-methylbutylamine (8). The benzyl ester protecting group was then removed by hydrogenolysis to give the desired peptide (phenylacetyl)-2(*S*)-malyl-5(*S*)-amino-4(*S*)-hydroxy-2(*S*)-isopropyl-7-(methyloctanoyl)-2(*S*)-methylbutylamine (XII).

To assess the effect of the carboxylic acid functionality at the P-2 site on the physical characteristics of the resulting peptides, the log PC values for peptides I and X were measured at *pH 7.4*. Histidine-containing peptide

(11) Symbols and abbreviations as recommended by the IUPAC-IUB Joint Commission on Biochemical Nomenclature: *Eur. J. Biochem.* **1984**, *138*, 9; the abbreviation Ψ(χ) indicates that χ replaces the amide –CONH– unit. Cal = cyclohexylalanine; Mal = (*S*)-malic acid; Amp = 2-(aminomethyl)pyridine; Mba = 2(*S*)-methylbutylamine; TBS = *tert*-butyldimethylsilyl; TFA = trifluoroacetic acid; DEPC = diethylphosphoryl cyanide; DMF = dimethylforamide; 1-HOBT = 1-hydroxybenzotriazole; DMAP = 4-(*N*,*N*-dimethylamino)pyridine.

(12) Thaisrivonga, S.; Pals, D. T.; Harris, D. W.; Kati, W. M.; Turner, S. R. *J. Med. Chem.* **1987**, *30*, 536. For synthesis of Boc-LeuΨ[CHOTBSCH$_2$]Val-OH see: Hester, J. B.; Pals, D. T.; Saneii, H. H.; Sawyer, T. K.; Schostarez, H. J.; TenBrink, R. E.; Thaisrivongs, S., European Patent Application, Publication Number 0173481, 1986.

I exhibited an apparent partition coefficient value of 2.7 while peptide X, with a carboxylic acid functional group, had a value of −0.22.

## Results on Renin Inhibition

These potential renin inhibitory peptides were tested in vitro against human plasma renin at pH 6 and their $IC_{50}$ values were determined as shown in Table I. As compared to the reference peptides I and V with histidine at the P-2 site, peptides II and VI with β-aspartic acid retained very high inhibitory potency. Congeneric peptide III with β-D-aspartic acid was less active than peptide II with β-L-aspartic acid. The cyclohexylmethyl side chain at P-1 has been shown to increase binding affinity of the resulting peptide over the isobutyl side chain of leucine.[13] Peptide IV with the cyclohexylalanine at P-1 site showed only a slight enhancement of potency over that of peptide II.

With the phenoxyacetyl N-terminal group, histidine-containing compound V showed much improved potency over peptide I. Peptides VI and VII also showed improved inhibitory potency over the phenylacetyl-containing peptides II and IV, respectively. The difference was more pronounced in the cyclohexylmethyl side-chain analogue VII, which exhibited an $IC_{50}$ value of 0.34 nM.

Interest in smaller C-terminal truncated peptides led us also to prepare compounds with 2(*S*)-methylbutylamide to mimic the isoleucine side chain at the P-2′ site. Peptides VIII and IX with β-aspartyl group at the P-2 site and 2(*S*)-methylbutylamine at the C-terminal end of the transition-state analogue inserts retained good inhibitory potency. As expected, the cyclohexylalanine at the P-1 site is more effective than the leucine residue, and peptide IX with molecular weight of 590 has an $IC_{50}$ value of 5.2 nM.

We also examined the oxygen analogue of β-aspartic acid at the P-2 site. Peptides X and XI with malic acid showed very high inhibitory potency. They are more active than the congeneric peptides II and VI, respectively, that contain β-aspartic acid at the P-2 site. This improvement in potency is more pronounced in the C-terminal truncated peptides containing 2(*S*)-methylbutylamide, and peptides XII, XIII, and XIV showed high renin inhibitory activities. Peptide XIII, for example, is 10 times more active than the β-aspartic acid containing peptide VIII. Peptide XII with molecular weight of 535 has an $IC_{50}$ value of 6 nM.

## Molecular Modeling Study

The molecular modeling study of human renin–inhibitor interactions in this work was based on a putative structure of human renin–substrate fragment complex as derived by Carlson. The original computer-assisted model of human renin,[10] without a bound ligand, was derived from the 3-D coordinates of several fungal aspartyl proteases since X-ray diffraction studies of *Rhizopus chinensis*, *Penicillium janthanellum*, and *Endothia parasitica*, which exhibited varying degrees of sequence homology to human renin, have been determined at a resolution of 1.8–3.0 Å. Recently, it was reported that the root mean square difference between the coordinates of the active site residues in a newly determined human renin structure and those of fungal aspartyl proteases was ca. 0.45 Å.[14] For the same set of residues, we have found the root mean square difference between the coordinates of *R. chinensis*[15] and that

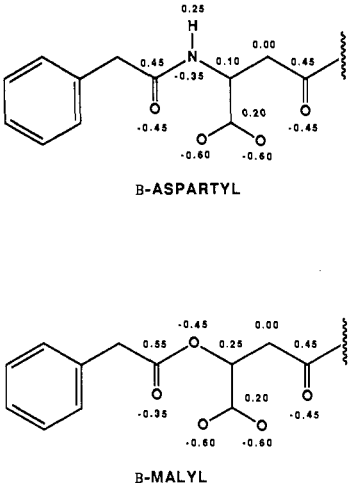


**Figure 1.** Atomic partial charges of the β-aspartic acid and malic acid moieties in the peptides for the purposes of energy minimization.

of this computer-assisted human renin model to be ca. 0.60 Å. This evidence is taken to support the close approximation of the previously derived human renin model, which was used in this study, to the recently determined coordinates of human renin. The octapeptide substrate fragment His-Pro-Phe-His-Leu-Val-Ile-His of the binary structure in the human renin–substrate complex was derived from the coordinates of pepstatin as bound to the aspartyl protease of *R. chinensis*.[16] A previous modeling study has shown that the structure of a bound substrate-based inhibitor could be constructed from this model of human renin–substrate fragment complex and that the conformation of this inhibitor is similar to the X-ray structure of the same inhibitor as bound to the *R. chinensis* enzyme.[17]

In this report, the coordinates of a substrate-based inhibitor were then generated by mapping atoms in the backbone of the inhibitor to those in the substrate fragment in analogous positions. The alignment of the backbone atoms began with the tripeptide subunit Leu-Val-Ile, and the coordinates of the backbone atoms in the inhibitor could be assigned. The side-chain atoms in this tripeptide subunit could also be mapped directly from the substrate fragment in an analogous fashion. For the residue at the P-2 site and the terminal residues, the side chains were mapped from the position of the substrate fragment as far as possible and the remaining coordinates were then generated with standard bond lengths and bond angles. The final side-chain dihedral angles were determined in the energy minimization of the resulting renin–inhibitor complex. For the minimization procedure using the CHARMM program,[18] a core region of the enzyme was defined to include all the residues that were located within a 14-Å distance from the bound inhibitor. All atoms lying outside of this core remained fixed in position, while the positions of the core atoms were adjusted by the ABNR procedure[18] in four 25-cycle steps, with successively reduced harmonic constraints of 20.0, 2.0, 0.2, and 0.02 kcal/mol. The

(13) Boger, J.; Payne, L. S.; Perlow, D. S.; Lohr, N. S.; Poe, M.; Blaine, E. H.; Ulm, E. H.; Schorn, T. W.; LaMont, B. I.; Lin, T.-Y.; Kawai, M.; Rich, D.; Veber, D. F. *J. Med. Chem.* **1985**, *28*, 1779.

(14) Sielecki, A. R.; Hayakawa, K.; Fujinaga, M.; Murphy, M. E. P.; Fraser, M.; Muir, A. K.; Carilli, C. T.; Lewicki, J. A.; Baxter, J. D.; James, M. N. G. *Science* **1989**, *243*, 346.

(15) Suguna, K.; Bott, R. R.; Padlan, E. A.; Subramanian, E.; Sheriff, S.; Cohen, G. H.; Davies, D. R. *J. Mol. Biol.* **1987**, *196*, 877.

(16) Bott, R.; Subramian, E.; Davies, D. R. *Biochemistry* **1982**, *21*, 6956.

(17) Sawyer, T. K.; Pals, D. T.; Mao, B.; Maggiora, L. L.; Staples, D. J.; deVaux, A. E.; Schostarez, H. J.; Kinner, J. H.; Smith, C. W. *Tetrahedron* **1988**, *44*, 661.

(18) Brooks, B. R.; Bruccoleri, R. E.; Olafson, B. D.; States, D. J.; Swaminathan, S.; Karplus, M. *J. Compt. Chem.* **1983**, *4*, 187.

electrostatic terms in the potential energy expression were calculated from Coulomb's law with a distance-dependent dielectric constant value $\epsilon$, which was assigned $\epsilon = r_{ij}$(where $r_{ij}$ is the distance in angstroms).[18] This treatment of electrostatic interactions is appropriate for enzyme–ligand subsite interactions within the interior of the complex. The partial charges assigned to the atoms in the β-aspartyl portion (Figure 1a) were consistent with those in an aspartic acid residue. In the malic acid analogue, the partial charges in the ester linkage were adjusted to reflect the higher electronegativity of the carboxylic oxygen. This adjustment, without more elaborate charge calculation, was suitable for our goals to investigate the overall interaction between the enzyme renin and the P-2 side chain. The electrostatic term in this interaction, in particular, was dominated by terms involving the large partial charges of the carboxylate oxygens (Figure 1a, and parts b).

The study of the interactions between the P-2 residue and the residues on the enzyme surface used the starting structure of an enzyme–inhibitor complex which had been energy-minimized as described above. With the rest of the complex in a fixed position, the P-2 residue was rotated, in 10-degree increments, for one full revolution about an axis that is defined by the two terminal backbone atoms of the residue. At each angular position, the structure of the complex was then refined by energy minimization. For computational purposes, a core region was defined to include all the residues of the enzyme within a 9-Å distance of either the P-2 residue of the inhibitor or the Thr-84 residue of the enzyme. Atoms outside of the core region remained fixed, while those within the core region were refined for a total of 100 ABNR cycles within three steps with successively reduced harmonic constraints of 5.0, 1.0, and 0.0 kcal/mol. As an approximation of the relative strength of binding affinity, the interaction energy ($E_{int}$) between the enzyme and the inhibitor, defined as $E_{complex} - E_{enzyme} - E_{inhibitor}$, was then calculated. The P-2 to Thr-84 separation, defined as the distances between the carboxylate oxygen atoms of the P-2 residue and the hydroxylic oxygen of Thr-84, was also computed after energy minimization of the complex for each angular position of the P-2 side chain.

Two epimeric β-aspartic acid containing inhibitors (compounds II and III) and one malic acid containing congener (compound X) were chosen for this study. An inhibitor with histidine at P-2 site (compound I) was also included for comparison; however, the imidazole ring was more bulky and was not rotated. The profile of $E_{int}$ for the 36 angular positions during the revolution of the P-2 residue of compound II about the backbone is shown in Figure 2a. The P-2 to Thr-84 distances for each position as defined earlier are also plotted. The carboxylic acid functionality of the P-2 residue is found close to the hydroxylic group of Thr-84 in the shaded region. In these positions, the $E_{int}$ is less favorable than that of the remaining region when the carboxylic acid functionality of the P-2 residue is located closer to the Ser-229 on the enzyme surface. Figure 2b displays a representative conformer of the inhibitor in each of the two regions. One conformer, which will be called the Thr-84 conformer, shows the carboxylic acid to be located within a hydrogen-bonding distance to the hydroxyl group of Thr-84 and in the other conformer (Ser-229 conformer), the carboxylic acid is hydrogen-bonded to the amide nitrogen of Ser-229. The carbonyl group of the phenylacetyl moiety is able to hydrogen-bond to the Thr-84 residue only in the Ser-229 conformer. Figure 3 compares the structure of compound II in the Ser-229 conformer with that of the reference

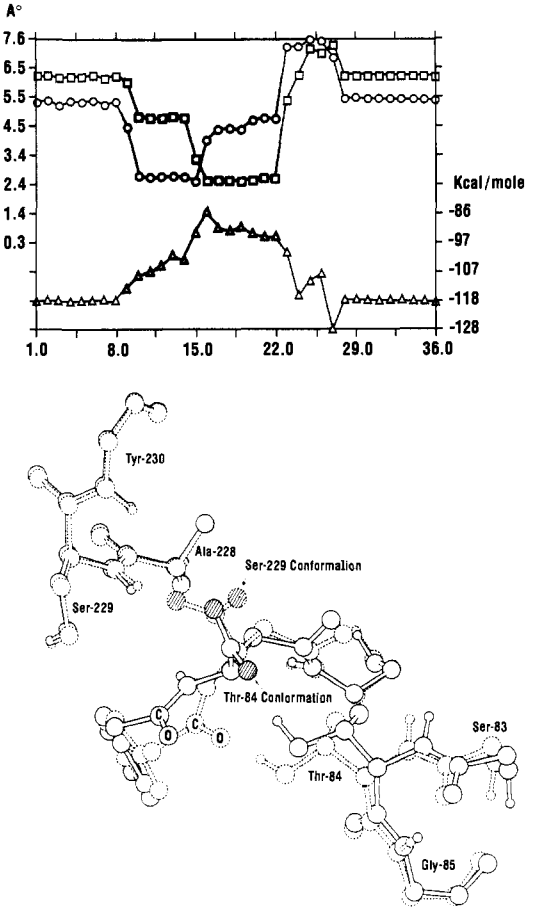


**Figure 2.** (a) The interaction energy ($E_{int}$) and the P-2 to Thr-84 distance profiles for the 36 angular positions of the P-2 side chain in compound II. The curve of the interaction energy is marked with triangles, and its values are indicated by the right ordinate. The distance curves, one for each of the two carboxylate oxygen to the Thr-84 hydroxyl oxygen distances, are marked with circles and squares and their values are indicated by the left ordinate. The shaded region represents conformations in which the carboxylate group is closer to the Thr-84 sidechain. (b) Two conformations of the P-2 side chain for compound II; each is a representative of the two regions shown in a. Also shown are two tripeptide units from the active site of renin, one containing the Ser-229 and the other Thr-84. The structure in solid lines is the Thr-84 conformation, in the shaded region in a, and the structure in dashed lines is the Ser-229 conformation. Shaded atoms are carboxylate oxygens of the P-2 side chain in each conformation.

**Table II.** The Interaction Energies of the β-Aspartic Acid Containing Compounds (II and III), the Malic Acid Containing Compound (X), and the Histidine-Containing Compound (I)

| compd | conformation | $E_{int}$, kcal/mol |
|---|---|---|
| II | Thr-84 | -92.9 |
| | Ser-229 | -127.9 |
| III | Thr-84 | -96.8 |
| | Ser-229 | -125.4 |
| X | Thr-84 | -100.5 |
| | Ser-229 | -117.6 |
| I | | -102.0 |

histidine-containing peptide (compound I). Similar observations of the Ser-229 and Thr-84 conformers can also be made qualitatively for compounds III and X. The $E_{int}$ and distances profiles for these two inhibitors are shown in Figures 4 and 5; $E_{int}$ are more favorable in the unshaded regions, where the carbonyl groups are located away from the Thr-84 and closer to Ser-229.

The characteristic $E_{int}$ in each of the two regions for these three inhibitors are listed in Table II. The favorable

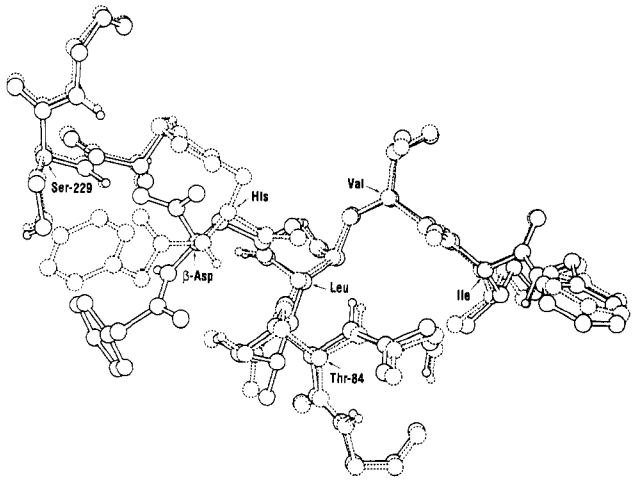


**Figure 3.** Comparison of the structure of compound II in the active site of renin in the Ser-229 conformation (solid lines) with the structure of the histidine analogue I (dashed lines). The two tripeptide units of the enzyme active site, shown in Figure 2b, are also included. The residue labels are placed at the $C_\alpha$ atoms of the respective residues.

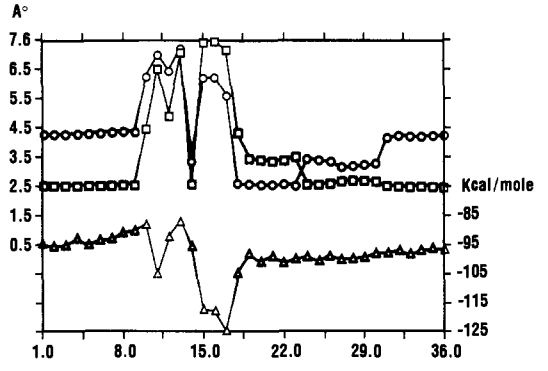


**Figure 4.** The interaction energy and the P-2 to Thr-84 distance profiles for the P-2 side chain in compound III. See Figure 2a for details.

conformers are the ones in which the carboxylic acid functionality is positioned closer to the serine-229 residue on the enzyme surface. The energy difference between the two conformers for compound X, however, is approximately $^1/_2$ of those for the aspartic acid containing analogues. This may suggest a more significant role for threonine-84 in the binding of the malic acid containing congener. For the lower energy conformers, the rank ordering of $E_{int}$ for the two aspartic acid containing inhibitors reflects their rank ordering of binding potency. $E_{int}$ for the lower energy conformer of compound X is somewhat higher than what might be anticipated from its relative binding potency as compared to the β-aspartic acid containing analogues. The smaller energy gap between the two conformers of compound X may lower the effective free energy of binding or this could simply be due to a disparity between the location of the inhibitors in the active site.

In summary, we have employed a reasonable model of human renin–substrate fragment complex in deriving the structures of several potent renin inhibitory peptides bound to the enzyme and devised a molecular modeling strategy to investigate the interaction of P-2 side chain with residues on the surface of renin binding pocket. In particular, the potential P-2 to Thr-84 interaction was investigated by calculating the interaction energy between renin and the inhibitors by a molecular mechanics energy function. The interaction energy was then compared to

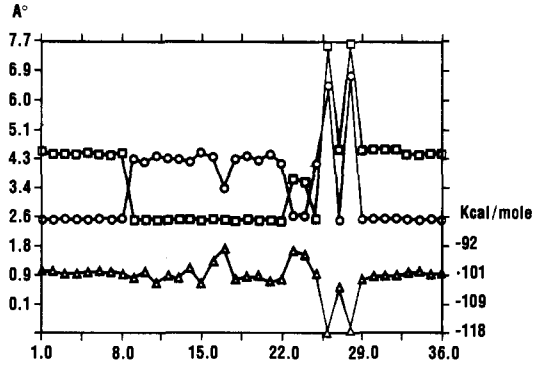


**Figure 5.** The interaction energy and the P-2 to Thr-84 distance profiles for the P-2 sidechain in compound IX. See Figure 2a for details.

the observed potency of renin inhibition of these peptides. It was found that, in addition to the conformation in which P-2 group interacts with Thr-84, there is another conformer for a carboxylate group at P-2 position in which it forms a hydrogen bond with Ser-229 amide group. Our results suggested that, excluding kinetic limitations, the Ser-229 conformer is more favorable, and also that, for the malic acid analogues, the P-2 to Thr-84 interaction may contribute to the binding of the inhibitor to renin and hence to its potency in enzyme inhibition.

## Conclusions

In this study, we were interested in taking advantage of the polar functionality on the surface of renin active site for potential hydrogen bonding with a polar functionality on the inhibitory ligand at the P-2 site. A β-aspartyl residue was chosen to replace the histidyl residue at this site in the peptide template. A series of renin inhibitory peptides were prepared to study the structure–activity relationship of of these β-aspartyl-containing peptides, with the hydroxyethylene isostere at the cleavage site. These compounds showed good renin inhibitory activities in the nanomolar range. Relatively small compound such as peptide IX with molecular weight of 590 exhibited good renin inhibitory potency. Another related series of renin inhibitory peptides were prepared in which malic acid was used in place of β-aspartic acid. The resulting peptides with the oxygen analogue showed improved renin inhibitory potency, especially in the smaller peptides. Relatively small compound such as peptide XII, with molecular weight of 535 and with no α-amino acid residue, retained good renin inhibitory activity. A molecular modeling study was also carried out to explore the possible mode of binding of these inhibitors to the active site of renin. Focusing on the potential interaction between the polar carboxylic functionality on the inhibitors and the functionality on Thr-84 or Ser-229 on the enzyme surface, the preferred enzyme-bound conformer of these inhibitors seems to be the one in which the carboxylic acid group is located close to Ser-229. Optimization of the compounds reported in this study to address the potential improvement of the biological activities in animal models is under current investigation.

## Experimental Section

Solvents were from Burdick & Jackson and used as received without further purification. Other reagents were obtained from Aldrich unless otherwise noted. Boc-protected amino acids were obtained from U. S. Biochem or Sigma. Diethyl ether was Mallinckrodt anhydrous grade. Dichloromethane for reactions was dried over 4A molecular sieves. Dimethylformamide was Aldrich gold-label grade and was stored over 4A sieves. Diisopropylethylamine was distilled from calcium hydride. Diethylphosphoryl cyanide was distilled before use. Thin-layer chro-

Table III. Physical Characteristics of Peptides

| compd[a] | HPLC[b] ($R_f$) | formula | FAB-HRMS calcd | FAB-HRMS found |
|---|---|---|---|---|
| I | 14.22 | $C_{38}H_{56}N_7O_5$ | 690.4343 | 690.4338 |
| II | 12.34 | $C_{36}H_{54}N_5O_7$ | 668.4023 | 668.4062 |
| III | 7.37 | $C_{36}H_{54}N_5O_7$ | 668.4023 | 668.4055 |
| IV | 7.47 | $C_{39}H_{58}N_5O_7$ | 708.4336 | 708.4328 |
| V | 13.9 | $C_{38}H_{56}N_7O_6$ | 706.4292 | 706.4290 |
| VI | 12.66 | $C_{36}H_{54}N_5O_8$ | 706.3792 | 706.3811 |
| VII | 7.13 | $C_{39}H_{58}N_5O_8$ | 724.4363 | 724.4339 |
| VIII | 25.6 | $C_{29}H_{48}N_3O_7$ | 550.3492 | 550.3498 |
| IX | 9.54 | $C_{32}H_{52}N_3O_7$ | 590.3805 | 590.3806 |
| X | 23.5 | $C_{36}H_{52}N_4O_8$ | 669.3863 | 669.3866 |
| XI | 23.8 | $C_{36}H_{53}N_4O_9$ | 685.3812 | 685.3824 |
| XII | 13.5 | $C_{29}H_{47}N_2O_7$ | 535.3383 | 535.3347 |
| XIII | 13.1 | $C_{29}H_{46}N_2O_8Na$ | 573.3152 | 573.3179 |
| XIV | 7.19 | $C_{32}H_{51}N_2O_8$ | 591.3645 | 591.3649 |

[a] $^1$H NMR was found to be consistent with the structures. [b] See the Experimental Section for conditions; $R_f$ is the retention time.

matography was performed on Merck precoated plates (silica gel 60, F-254). Column chromatography was performed with 70–230 mesh silica gel 60; for flash chromatography the 230–400 mesh grade was used.

Proton nuclear magnetic resonance ($^1$H NMR) spectra were recorded on a Bruker AM-300 (300 MHz) instrument, in deuterated chloroform unless otherwise noted. Mass spectra were performed by Physical and Analytical Chemistry of the Upjohn Company. High-pressure liquid chromatography was performed on a Perkin-Elmer Series IV liquid chromatograph operating at 1.5 mL/min using a Brownlee RP-18 10-μm column, with UV monitoring by a Kratos Spectroflow 773 detector, at 225 and 254 nm. A Perkin-Elmer LCI-100 integrator was used for peak data. Solvent A is methanol; solvent B is an aqueous phosphate pH 3 buffer (5.22 g of $NaH_2PO_4$ monohydrate and 0.76 mL of 85% phosphoric acid in 4 L of Burdick & Jackson water); solvent C is 0.1% trifluoroacetic acid in 90% water and 10% acetonitrile; solvent D is 0.1% trifluoroacetic acid in 10% water and 90% acetonitrile; solvent E is 90% aqueous phosphate pH 3 buffer and 10% acetonitrile; solvent F is 80% acetonitrile, 10% tetrahydrofuran, and 10% aqueous phosphate pH 3 buffer. The solvent system for peptides IV, VII, IX, and XIV is 70% solvent A and 30% solvent B. The solvent system for peptide III is 65% solvent A and 35% solvent B. The solvent system for peptides II and VI is 60% solvent A and 40% solvent B. Solvent system for peptide I is 10% solvent C and 90% solvent D. Solvent system for peptides XII and XIII is 60% solvent C and 40% solvent D. Solvent system for peptides VIII, X, and XI is 70% solvent C and 30% solvent D. Peptide V was analyzed on a 5 μm column at a flow rate of 2 mL/min with a gradient of 25% solvent E and 75% solvent F to 100% solvent F in 20 min. See Table III for the physical characteristics of the peptides.

**(Phenylacetyl)-$N^{im}$-tosyl-L-histidyl-5(*S*)-amino-4(*S*)-hydroxy-2(*S*)-isopropyl-7-(methyloctanoyl)-L-isoleucyl-2-pyridylmethylamine (3).** A solution of 60 mg (0.073 mmol) of (*tert*-butyloxycarbonyl)-$N^{im}$-tosyl-L-histidyl-5(*S*)-amino-4(*S*)-hydroxy-2(*S*)-isopropyl-7-(methyloctanoyl)-L-isoleucyl-2-pyridylmethylamine (**2**)[12] in 0.25 mL of dichloromethane and 0.25 mL of trifluoroacetic acid was allowed to stir for 45 min. The reaction mixture was slowly added to a stirred solution of 0.5 g of $NaHCO_3$ in 10 mL of water. The resulting mixture was extracted with several portions of dichloromethane containing a small amount of methanol. The combined organic phase was dried ($MgSO_4$) and then concentrated to give 50 mg (0.069 mmol) of the corresponding amine.

To a stirred solution of this amine and 12 mg (0.088 mmol) of phenylacetic acid in 0.5 mL of dichloromethane and 0.5 mL of dimethylformamide were added 30 μL (0.17 mmol) of diisopropylethylamine and 14 μL (0.092 mmol) of diethylphosphoryl cyanide.[19] After stirring at room temperature overnight, the solvents were removed under reduced pressure, and the resulting residue was chromatographed on silica gel with 5%–7% methanol in dichloromethane to give 53 mg (0.063 mmol, 86%) of (phenylacetyl)-$N^{im}$-tosyl-L-histidyl-5(*S*)-amino-4(*S*)-hydroxy-2(*S*)-isopropyl-7-(methyloctanoyl)-L-isoleucyl-2-pyridylmethylamine (**3**): $^1$H NMR ($CDCl_3$) δ 0.7–0.9 (m, 18 H), 2.4 (s, 3 H), 3.5 (s, 2 H), 7.1–7.3 (m, 9 H), 7.35 (d, $J$ = 8 Hz, 2 H), 7.75 (d, $J$ = 8 Hz, 2 H), 7.8 (s, 1 H), 8.45 (d, $J$ = 5 Hz, 1 H); HRMS $m/z$ 844.4445 (calcd for $C_{45}H_{62}N_7O_7S$, 844.4431).

**(Phenylacetyl)-L-histidyl-5(*S*)-amino-4(*S*)-hydroxy-2(*S*)-isopropyl-7-(methyloctanoyl)-L-isoleucyl-2-pyridylmethylamine (I).** A solution of 50 mg (0.059 mmol) of (phenylacetyl)-$N^{im}$-tosyl-L-histidyl-5(*S*)-amino-4(*S*)-hydroxy-2(*S*)-isopropyl-7-(methyloctanoyl)-L-isoleucyl-2-pyridylmethylamine (**3**) and 45 mg (0.3 mmol) of 1-hydroxybenzotriazole in 0.5 mL of methanol was allowed to stir at room temperature overnight. The reaction mixture was concentrated under reduced pressure and the resulting residue was chromatographed on silica gel with 7% methanol (saturated with ammonia) in dichloromethane to give 21 mg (0.03 mmol, 52%) of (phenylacetyl)-L-histidyl-5(*S*)-amino-4(*S*)-hydroxy-2(*S*)-isopropyl-7-(methyloctanoyl)-L-isoleucyl-2-pyridylmethylamine (I): $^1$H NMR ($CDCl_3$) δ 0.7–0.9 (m, 18 H), 3.5 (b s, 2 H) 6.6 (s, 1 H), 7.1–7.35 (m, 7 H), 7.4 (s, 1 H), 7.6 (m, 1 H), 8.4 (d, $J$ = 5 Hz, 1 H); HRMS $m/z$ 690.4338 (calcd for $C_{38}H_{56}N_7O_5$, 690.4343).

**(*tert*-Butyloxycarbonyl)-α-benzyl-β-L-aspartyl-5(*S*)-amino-4(*S*)-hydroxy-2(*S*)-isopropyl-7-(methyloctanoyl)-L-isoleucyl-2-pyridylmethylamine (4).** To a stirred solution of 380 mg (0.58 mmol) of (*tert*-butyloxycarbonyl)-5(*S*)-amino-4(*S*)-[(*tert*-butyldimethylsilyl)oxy]-2(*S*)-isopropyl-7-(methyloctanoyl)-L-isoleucyl-2-pyridylmethylamine (**1**)[7] in 5 mL of ether was added gaseous hydrogen chloride. After stirring for 15 min, the solvent was removed by a stream of nitrogen and the resulting residue was dried under reduced pressure.

To a stirred mixture of this solid residue and 157 mg (0.485 mmol) of (*tert*-butyloxycarbonyl)-α-benzyl-β-L-aspartic acid in 2 mL of dichloromethane were added 0.36 mL (2.0 mmol) of diisopropylethylamine and 0.10 mL (0.65 mmol) of diethylphosphoryl cyanide. The resulting mixture was allowed to stir at room temperature overnight. It was partitioned between aqueous $NaHCO_3$ and dichloromethane. The organic phase was dried ($MgSO_4$) and then concentrated. The residue was chromatographed on silica gel with 5% methanol in dichloromethane to give 332 mg (0.45 mmol, 93%) of (*tert*-butyloxycarbonyl)-α-benzyl-β-L-aspartyl-5(*S*)-amino-4(*S*)-hydroxy-2(*S*)-isopropyl-7-(methyloctanoyl)-L-isoleucyl-2-pyridylmethylamine (**4**): $^1$H NMR ($CDCl_3$) δ 0.8–0.9 (m, 18 H), 1.41 (s, 1 H), 5.16 (b s, 2 H), 7.2 (m, 1 H), 7.2–7.4 (m, 6 H), 7.6 (m, 1 H), 8.5 (d, $J$ = 5 Hz, 1 H); HRMS $m/z$ 740.4616 (calcd for $C_{40}H_{62}N_5O_8$, 740.4598).

**(Phenylacetyl)-α-benzyl-β-L-aspartyl-5(*S*)-amino-4(*S*)-hydroxy-2(*S*)-isopropyl-7-(methyloctanoyl)-L-isoleucyl-2-pyridylmethylamine (5).** A solution of 747.5 mg (1.0 mmol) of (*tert*-butyloxycarbonyl)-α-benzyl-β-L-aspartyl-5(*S*)-amino-4(*S*)-hydroxy-2(*S*)-isopropyl-7-(methyloctanoyl)-L-isoleucyl-2-pyridylmethylamine (**4**) in 2 mL of dichloromethane and 2 mL of trifluoroacetic acid was allowed to stir at room temperature for 45 min. The reaction mixture was slowly added to a stirred solution of 3 g of $NaHCO_3$ in 30 mL of water. The resulting mixture was extracted with several portions of dichloromethane. The combined organic phase was dried ($MgSO_4$) and then concentrated to give 641.3 mg (1.0 mmol) of the corresponding free amine.

To a stirred solution of 425.6 mg (0.67 mmol) of this residue and 117.8 mg (0.86 mmol) of phenylacetic acid in 3 mL of dichloromethane were added 0.24 mL (1.39 mmol) of diisopropylethylamine and 0.16 mL (1.06 mmol) of diethylphosphoryl cyanide. The resulting mixture was allowed to stir overnight and then partitioned between aqueous $NaHCO_3$ and dichloromethane. The organic phase was dried ($MgSO_4$) and then concentrated. The residue was chromatographed on silica gel with 5% methanol in dichloromethane to give 322.6 mg (0.426 mmol, 64%) of (phenylacetyl)-α-benzyl-β-L-aspartyl-5(*S*)-amino-4(*S*)-hydroxy-2(*S*)-isopropyl-7-(methyloctanoyl)-L-isoleucyl-2-pyridylmethylamine (**5**): $^1$H NMR ($CDCl_3$) δ 0.8–0.9 (m, 18 H), 3.6 (s, 2 H), 5.1 (b s, 2 H), 7.2–7.4 (m, 12 H), 7.7 (m, 1 H), 8.5 (d, $J$ = 5 Hz, 1 H); HRMS $m/z$ 758.4505 (calcd for $C_{43}H_{60}N_5O_7$, 758.4492).

**(Phenylacetyl)-β-L-aspartyl-5(*S*)-amino-4(*S*)-hydroxy-2(*S*)-isopropyl-7-(methyloctanoyl)-L-isoleucyl-2-pyridylmethylamine (II).** To a stirred suspension of 120 mg (0.158

(19) Yamada, S.; Kasai, Y.; Shioiri, T. *Tetrahedron Lett* **1973**, 1595.

mmol) of (phenylacetyl)-α-benzyl-β-L-aspartyl-5(*S*)-amino-4(*S*)-hydroxy-2(*S*)-isopropyl-7-(methyloctanoyl)-L-isoleucyl-2-pyridylmethylamine (**5**) in 2 mL of dimethylformamide was added 75 mg of 10% palladium on charcoal, followed by 109.5 mg (1.73 mmol) of ammonium formate. After stirring at room temperature for 3 h, the mixture was diluted with methanol and then filtered through Celite with methanol washings. The filtrate was concentrated and the resulting residue was then chromatographed on silica gel with 20% methanol in dichloromethane to give 100 mg (0.15 mmol, 95%) of (phenylacetyl)-β-L-aspartyl-5(*S*)-amino-4(*S*)-hydroxy-2(*S*)-isopropyl-7-(methyloctanoyl)-L-isoleucyl-2-pyridylmethylamine (II): $^1$H NMR ($CDCl_3$) δ 0.8–0.9 (m, 18 H), 3.6 (s, 2 H), 7.2–7.4 (m, 7 H), 7.7 (m, 1 H), 8.5 (d, $J$ = 5 Hz, 1 H); HRMS $m/z$ 668.4062 (calcd for $C_{38}H_{54}N_5O_7$, 668.4023).

**(*tert*-Butyloxycarbonyl)-5(*S*)-amino-4(*S*)-[(*tert*-butyldimethylsilyl)oxy]-2(*S*)-isopropyl-7-(methyloctanoyl)-2(*S*)-methylbutylamine (6).** To a stirred solution of 1.78 g (4.0 mmol) of 4(*S*)-[(*tert*-butyldimethylsilyl)oxy]-5(*S*)-[(*tert*-butyloxycarbonyl)amino]-2(*S*)-isopropyl-7-methyloctanoic acid[7] and 0.57 mL (4.8 mmol) of 2(*S*)-methylbutylamine were added 0.84 mL (4.8 mmol) of diisopropylethylamine and 0.74 mL (4.8 mmol) of diethylphosphoryl cyanide. After stirring at room temperature for 6 h, the reaction mixture was concentrated and the residue was chromatographed on silica gel with 20% ethyl acetate in hexane to give 2.0 g (3.88 mmol, 97%) of (*tert*-butyloxycarbonyl)-5(*S*)-amino-4(*S*)-[(*tert*-butyldimethylsilyl)oxy]-2(*S*)-isopropyl-7-(methyloctanoyl)-2(*S*)-methylbutylamine (**6**): $^1$H NMR ($CDCl_3$) δ 0.08 (s, 3 H), 0.09 (s, 3 H), 0.8–1.0 (m, 27 H), 1.42 (s, 9 H), 1.0–2.1 (m, 10 H), 2.95 (m, 1 H), 3.2 (m, 1 H), 3.65 (m, 2 H), 4.52 (d, $J$ = 10 Hz, 1 H), 5.72 (t, $J$ = 6 Hz, 1 H); HRMS $m/z$ 515.4235 (calcd for $C_{28}H_{59}N_2O_4Si$, 515.4244).

**1-Benzyl-2(*S*)-malyl-5(*S*)-amino-4(*S*)-[(*tert*-butyldimethylsilyl)oxy]-2(*S*)-isopropyl-7-(methyloctanoyl)-2(*S*)-methylbutylamine (7).** A solution of 215 mg (0.42 mmol) of (*tert*-butyloxycarbonyl)-5(*S*)-amino-4(*S*)-[(*tert*-butyldimethylsilyl)oxy]-2(*S*)-isopropyl-7-(methyloctanoyl)-2(*S*)-methylbutylamine (**6**) in 0.5 mL of dichloromethane and 0.5 mL of trifluoroacetic acid was allowed to stir at room temperature for 45 min. The mixture was slowly added to a stirred solution of 1 g of $NaHCO_3$ in 10 mL of water. The resulting mixture was extracted with several portions of dichloromethane. The combined organic phase was dried ($MgSO_4$) and then concentrated to give 173 mg (0.42 mmol).

To a stirred solution of this residue and 112 mg (0.50 mmol) of 1-benzyl-(*S*)-malic acid in 2 mL dichloromethane were added 87 μL (0.50 mmol) of diisopropylethylamine and 77 μL (0.50 mmol) of diethylphosphoryl cyanide. After stirring at room temperature overnight, the reaction mixture was concentrated and the resulting residue was then chromatographed on silica gel with 20% ethyl acetate in dichloromethane to give 127 mg (0.21 mmol, 49%) of 1-benzyl-2(*S*)-malyl-5(*S*)-amino-4(*S*)-[(*tert*-butyldimethylsilyl)oxy]-2(*S*)-isopropyl-7-(methyloctanoyl)-2(*S*)-methylbutylamine (**7**): $^1$H NMR ($CDCl_3$) δ 0.10 (s, 3 H), 0.11 (s, 3 H), 0.8–0.95 (m, 15 H), 5.15 (d, $J$ = 12 Hz, 1 H), 5.25 (d, $J$ = 12 Hz, 1 H), 7.35 (b s, 5 H); HRMS $m/z$ 621.4273 (calcd for $C_{34}H_{61}N_2O_6Si$, 621.4299).

**(Phenylacetyl)-1-benzyl-2(*S*)-malyl-5(*S*)-amino-4(*S*)-[(*tert*-butyldimethylsilyl)oxy]-2(*S*)-isopropyl-7-(methyloctanoyl)-2(*S*)-methylbutylamine (8).** To a stirred solution of 65 mg (0.10 mmol) of 1-benzyl-2(*S*)-malyl-5(*S*)-amino-4(*S*)-[(*tert*-butyldimethylsilyl)oxy]-2(*S*)-isopropyl-7-(methyloctanoyl)-2(*S*)-methylbutylamine (**7**) and 26 mg (0.21 mmol) of 4-(dimethylamino)pyridine in 1 mL of dichloromethane was added 17 μL (0.13 mmol) of phenylacetyl chloride. After stirring at room temperature overnight, the concentrated reaction mixture was chromatographed on silica gel with 8% ethyl acetate in dichloromethane to give 56.3 mg (0.073 mmol, 73%) of (phenylacetyl)-1-benzyl-2(*S*)-malyl-5(*S*)-amino-4(*S*)-[(*tert*-butyldimethylsilyl)oxy]-2(*S*)-isopropyl-7-(methyloctanoyl)-2(*S*)-methylbutylamine (**8**): $^1$H NMR δ 0 (2 s, 2 × 3 H), 0.7–0.9 (m, 18 H), 3.55 (s, 2 H), 5.39 (d, $J$ = 9 Hz, 1 H), 5.41 (d, $J$ = 9 Hz, 1 H), 7.1–7.3 (m, 10 H); HRMS $m/z$ 739.4692 (calcd for $C_{42}H_{67}N_2O_7Si$, 739.4717).

**(Phenylacetyl)-2(*S*)-malyl-5(*S*)-amino-4(*S*)-hydroxy-2(*S*)-isopropyl-7-(methyloctanoyl)-2(*S*)-methylbutylamine (XII).** A solution of 56.3 mg (0.076 mmol) of (phenylacetyl)-1-benzyl-2(*S*)-malyl-5(*S*)-amino-4(*S*)-[(*tert*-butyldimethylsilyl)oxy]-2(*S*)-isopropyl-7-methyloctanoyl-2(*S*)-methylbutylamine (**8**) in 0.25 mL of dichloromethane and 0.25 mL of trifluoroacetic acid was allowed to stir at room temperature for 1 h. The reaction mixture was partitioned between aqueous $NaHCO_3$ and dichloromethane. The organic phase was dried ($MgSO_4$) and then concentrated to give 50 mg of (phenylacetyl)-1-benzyl-2(*S*)-malyl-5(*S*)-amino-4(*S*)-hydroxy-2(*S*)-isopropyl-7-(methyloctanoyl)-2(*S*)-methylbutylamine.

A mixture of this residue and 20 mg of 5% palladium on charcoal in 1 mL of methanol was shaken under 50 psi of hydrogen for 2 h. The reaction mixture was filtered through Celite with methanol washings. The filtrate was concentrated and the resulting residue was chromatographed on silica gel with 10% methanol in dichloromethane to give 26.7 mg (0.05 mmol, 66%) of (phenylacetyl)-2(*S*)-malyl-5(*S*)-amino-4(*S*)-hydroxy-2(*S*)-isopropyl-7-(methyloctanoyl)-2(*S*)-methylbutylamine (XII): $^1$H NMR ($CDCl_3$) δ 0.8–0.9 (m, 18 H), 3.65 (b s, 2 H), 7.1–7.3 (m, 5 H); HRMS $m/z$ 535.3347 (calcd for $C_{29}H_{47}N_2O_7$, 535.3383).

**Biology. Inhibition of Human Plasma Renin.** These peptides were assayed for plasma renin inhibitory activity as follows: Lyophilized human plasma with 0.1% EDTA was obtained commercially (New England Nuclear). The angiotensin I generation step utilized 250 μL of plasma, 2.5 μL of phenylmethanesulfonyl fluoride, 25 μL of maleate buffer (pH 6.0), and 10 μL of an appropriate concentration of peptide in a 1% Tween 80 in water vehicle. Incubation was for 90 min at 37 °C. Radioimmunoassay for angiotensin I was carried out with a commercial kit (Clinical Assays). Plasma renin activity values for tubes with peptide were compared to those for control tubes to estimate percent inhibition. The inhibition results were expressed as $IC_{50}$ values, which were obtained by plotting three or four peptide concentrations on semilog graph paper and estimating the concentration producing 50% inhibition.

**Acknowledgment.** We would like to thank Dr. Jackson B. Hester for compound V and we also are grateful to Margaret R. Shuette and Lisa A. Foellmi for technical assistance.